ARTICLE

Toward All-Carbon Electronics: Fabrication of Graphene-Based Flexible Electronic Circuits and Memory Cards Using Maskless Laser Direct Writing

Jiajie Liang,[†] Yongsheng Chen,[*,†] Yanfei Xu,[†] Zhibo Liu,[*,‡] Long Zhang,[†] Xin Zhao,[‡] Xiaoliang Zhang,[‡] Jianguo Tian,[‡] Yi Huang,[†] Yanfeng Ma,[†] and Feifei Li[†]

Key Laboratory of Functional Polymer Materials and Center for Nanoscale Science & Technology, Institute of Polymer Chemistry, College of Chemistry, Nankai University, Tianjin 300071, China, and Key Laboratory of Weak Light Nonlinear Photonics Ministry of Education and Teda Applied Physics School, Nankai University, Tianjin 300457, China

ABSTRACT Owing to its extraordinary electronic property, chemical stability, and unique two-dimensional nanostructure, graphene is being considered as an ideal material for the highly expected all-carbon-based micro/nanoscale electronics. Herein, we present a simple yet versatile approach to constructing all-carbon micro/nanoelectronics using solution-processing graphene films directly. From these graphene films, various graphene-based microcosmic patterns and structures have been fabricated using maskless computer-controlled laser cutting. Furthermore, a complete system involving a prototype of a flexible write-once-read-many-times memory card and a fast data-reading system has been demonstrated, with infinite data retention time and high reliability. These results indicate that graphene could be the ideal material for fabricating the highly demanded all-carbon and flexible devices and electronics using the simple and efficient roll-to-roll printing process when combined with maskless direct data writing.

KEYWORDS: all-carbon micro/nanoelectronics • graphene film • flexible • maskless • laser direct writing • memory card

INTRODUCTION

Graphene is emerging as a novel two-dimensional (2-D) material in the field of materials science owing to its prominent intrinsic electronic (1, 2), thermal (3), mechanical (4, 5), structural (6, 7) and chemical (8) properties in recent years. These combined unique and intriguing features have spurred worldwide research aimed at plentiful potential applications such as nanocomposites (9−14), transparent conducting films (15−21), sensors (22−25), supercapacitors (26, 27), batteries (28), and so on. More importantly, new and higher expectations for the search of low-cost and flexible all-carbon devices or integrated circuits (ICs) have been generated because of this newly discovered and exciting 2-D material (29, 30). However, to fully realize its potential for most of the proposed graphene-based devices, one key is to develop an easy method to fabricate a patterned graphene film (or single graphene sheet) at the micro or nanoscale level, as needs to done with silicon for various silicon-based electronic components (31, 32). To date, different methods, including thermal graphitization or chemical vapor deposition with a prepatterned catalyst on substrates and a microcontact printing technique, have been explored to fabricate graphene-based nanoelectronics (30, 33−36). Albeit, all of these approaches require conventional lithographic techniques, high temperature, or a predefined patterned mask, which have disadvantages such as high production cost, low manufacturing yield, high time consumption, environmental pollution, and/or precluding the use of flexible plastics as substrates for device fabrication.

Among the current methods to produce graphene materials, wet chemistry utilizing chemical oxidation and intercalation is an easy and effective way to prepare graphene oxide (GO) in large quantities (15, 37). These GO materials can be dispersed homogeneously in water at the state of completely individual sheet level (38−40). This makes it possible to generate a continuous and uniform graphene-based film on various substrates, such as glass, quartz, and flexible polymer substrates, using the solution spin-coating process applicable for low-cost and roll-to-roll device fabrication. Nevertheless, the introduction of the functional groups as well as the damaged aromatic framework to GO renders this material electrically insulated, thus limiting its direct device applications. Fortunately, with controlled chemical reduction and/or thermal annealing conditions, most of the functional groups and defects on GO can be removed and the graphene intrinsic structure along with excellent electrical properties can be largely restored (15). Therefore, combined with

* To whom correspondence should be addressed. E-mail: yschen99@nankai.edu.cn (Y.C.), rainingstar@nankai.edu.cn (Z.L.).
Received for review August 14, 2010 and accepted October 26, 2010
† Key Laboratory of Functional Polymer Materials and Center for Nanoscale Science & Technology, Institute of Polymer Chemistry, College of Chemistry.
‡ Key Laboratory of Weak Light Nonlinear Photonics Ministry of Education and Teda Applied Physics School.
DOI: 10.1021/am1007326

Published on Web 11/08/2010

control of the electrical state of graphene (such as opening its band gap), it is possible to build all-carbon electrical devices and ICs using only graphene.

Lately, the advanced technique of laser direct cutting, which has the advantages of maskless, rapid prototyping, reliability, amenability, upward scalability, and low cost (41−43), is of increasing importance in device fabrication and has been used to construct microstructures on various films of semiconductor, metal, and dielectric polymer (44−49). Various accurate and complex architectures can be fabricated through the computer-controlled laser beam. However, it is still a big step away using this technique to meet the need for fabricating the real-world micro/nano-electronic circuits and devices. To date, two key issues remain for this technique. First, the silicon-based semiconducting microstructures fabricated with the laser-writing technique make it rather difficult to have a clean structure and thus are unusable because of the nonvolatile remains (45, 48). Second, as to the fabrication of organic or polymer films using this technique, their relatively poor chemical stability and resistance likewise extremely handicap their further use in this field. Herein, we describe a maskless process to fabricate all-carbon electronic circuits using a continuous graphene film prepared from a graphene solution spin-coating process followed by maskless laser writing. For the first time, we demonstrate that various graphene-based patterns and micro/nanostructures can be cleanly and regularly fabricated using this maskless fabrication with laser direct writing. Of great significance is that this writing process could be operated directly in air at ambient conditions, and various patterns used for electrical circuits and devices can be easily achieved. On this basis, a novel prototype of write-once-read-many-times (WORM) memory cards (fabricated on flexible polyimide, quartz, and glass substrates) along with a data-retrieving system has been demonstrated. Remarkably, owing to the extraordinary chemical stability of graphene, these graphene-based WORM memory cards possess almost infinite data retention time and extreme reliability, which are crucial in the practical use of some memory devices, such as identification cards, radio-frequency tags, passports, e-tickets, and military applications. Given the current laser direct-writing technology and the easy solution processing for graphene materials, it is fully expected that various all-carbon electronic circuits and devices can be facilely fabricated with this approach.

EXPERIMENTAL SECTION

Synthesis of Graphene Oxide (GO). GO prepared from natural graphite by the modified Hummer's method (15, 37) is used as the starting material to fabricate a high-quality graphene film.

Substrate Preparation and Fabrication of GO Films. Glass and quartz slides were cleaned in an ultrasonic bath with detergent, deionized water, acetone, and isopropyl alcohol, respectively, followed by extensive rinsing with deionized water, drying under a nitrogen stream, and storage in a vacuum oven at 80 °C until use, typically within a period of 2 h. Polyimide (PI) strips were ultrasonicated in ethanol for 30 min, followed by drying under a nitrogen stream and storage in a vacuum oven at 60 °C until use, typically within a period of 1 h. Aqueous solutions of GO with different concentrations were deposited on the prepared substrates and allowed to wet the surface for 1 min, after which the slide was allowed to spin at 700 rpm for 12 s to cause uniform spreading of the solution on the substrate and then at 2000 rpm for 1 min to dry the film. Films were further dried by placing them in a vacuum oven at 80 °C for 3 h before any reducing treatments. The thickness of the films was controlled by the concentration of the solutions. Given the need for an excellent continuous graphene film without any cracks for nanoelectronics, the concentration of the GO solution should be larger than 1 mg/mL. For fabrication of all our memory devices and graphene-based patterns in this paper, we chose a concentration of 5 mg/mL for both aqueous solutions of GO, and the thickness of these spin-coated films is about 40 nm measured by a film-thickness measuring device (AMBious Xp-2).

Hydrazine Vapor Reduction and Thermal Annealing. Either hydrazine chemical reduction or high-temperature annealing is an effective method to restore the electrical conductivity of graphene. When reduced by utilizing hydrazine, GO films on slides were placed in a perfectly cleaned glass Petri dish inside a larger glass Petri dish, which also contained 1 mL of hydrazine hydrate (80%; Tianjin Ruijinte Chemical Co., Ltd.). The larger dish was covered with a glass lid, sealed with Parafilm tape, and reduced at 40 °C for 1 day, after which the dish was opened and the films were rinsed with purified water and dried both under a nitrogen stream and by heating to 80 °C in a vacuum. For reduction using thermal annealing, dry GO films on slides were loaded into the tube furnace. Films were heated under a continuous flow of an ultrapure argon/H_2 mixture (95:5), at a rate of 5 °C/min, held at the desired temperature for 2 h, and then allowed to cool to room temperature. For all of our samples, we selected 400 °C as the annealing temperature because it is a widely used condition and our PI substrate can also resist such an annealing temperature. For fabrication of the 10 bits of WORM devices, 10 pairs of gold electrode with 50 nm were thermally evaporated under a vacuum onto the reduced graphene film through a copper-grid mask.

Laser Cutting and Writing. The procedures of laser-cutting bits and writing information were all implemented through a regeneratively amplified Ti:sapphire laser system (Spitfire Pro XP from Spectra-Physics) with a central wavelength of 800 nm, a pulse duration of 120 fs, and a repetition rate of 1 kHz used as the writing laser. The beam was incident onto an objective lens (Olympus, LMPlanFL). The magnification of the objective lens was 20×. The sample was mounted on computer-controlled translation and rotation stages. The movement of the stages made the focus of the femtosecond laser pulses scan through the sample. The output from our femtosecond laser was a Gaussian beam (TEM00 mode).

Electrical Measurements. The conductivity of the graphene films and electrical current of the memory cards were measured using a Keithley 2400 instrument.

RESULTS AND DISCUSSION

Solution processing is a highly demanded and low-cost technique for the fabrication of various organic/polymer materials-based devices because it can use the conventional roll-to-roll printing process on flexible substrates. In this work, we started by first preparing the continuous and uniform electrical conductive graphene films with high quality using the solution spin-coating means according to our previous works (15). In brief, GO was first completely exfoliated down to individual sheets in distilled water to form a stable dispersion of the GO solution. This GO dispersion was then spin-coated on the clean glass, quartz, or flexible PI substrates to form an integrated GO film. In practice, this

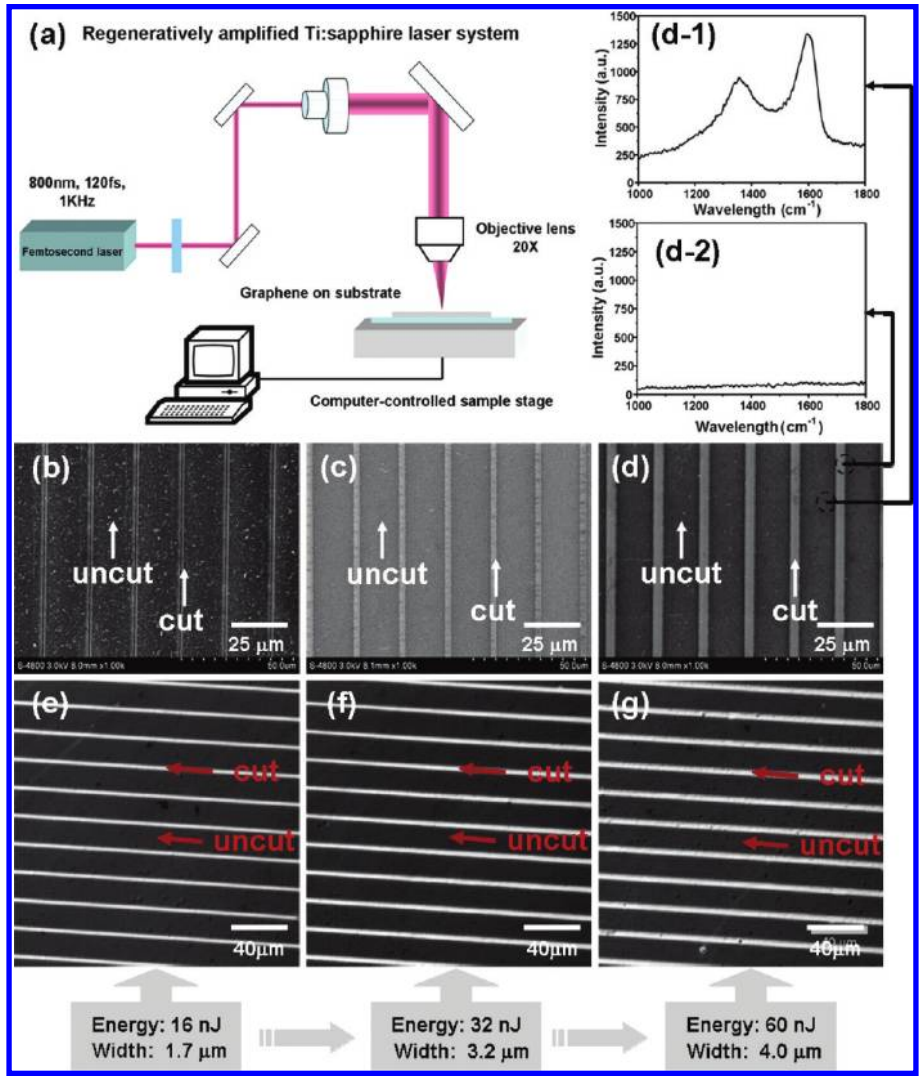

FIGURE 1. (a) Schematic illustration of the setup for the laser system used in this work. (b) SEM image of the channel pattern for the graphene film on flexible PI. The dark- and light-gray areas correspond to uncut and cut regions, respectively. (c) SEM image of the channel pattern for the graphene film on glass. The dark- and light-gray areas correspond to uncut and cut regions, respectively. (d) SEM image of the channel pattern for the graphene film on quartz. The dark- and light-gray areas correspond to uncut and cut regions, respectively. The exposure energy used in parts b–d is all 16 nJ. (d-1) Raman spectra of the uncut area for the graphene film on quartz. (d-2) Raman spectra of the cut area for the graphene film on quartz. The Raman results show that all graphene materials are cleaning etched away in the trenches after laser direct cutting. (e–g) Optical microscope images of the channel patterns for graphene films on quartz cut under different exposure energies. The dark- and light-gray areas correspond to uncut and cut regions, respectively. The exposure energy used in part e is 16 nJ, and the width for the cut channels is about 1.7 μm; the exposure energy used in part f is 32 nJ, and the width for the cut channels is about 3.2 μm; the exposure energy used in part g is 60 nJ, and the width for the cut channels is about 4.0 μm.

solution spin-coating process is suitable for almost all substrates, particularly flexible and large-area polymer-based substrates. The thickness of these GO films can also be controlled easily by the spin-coating speed and the concentration of the GO solution. Then, for the purpose of rendering this insulating GO film electrically conductive, hydrazine reduction and/or thermal annealing is (are) applied to restore its graphitic network structure (15). Except as noted, the concentration of the GO solution used in experiments is 5 mg/mL (see methods for details), and the obtained thickness of the graphene films is approximately 40 nm (as determined from the film-thickness measuring device). It has been extensively investigated that chemical reduction could only partially recover the conductivity of the graphene film, and the electrical performance can be enhanced further with an increase in the annealing temperature (15). This means that the electrical conductivity of the graphene-based films and, further, their electrical device can be easily tuned through control of the reduction conditions. This tunable electrical performance for graphene-based films, which cannot be easily achieved by either metal or conducting polymer films, is highly important for satisfying different requirements for device applications. In fact, from the economic point of view, the conductivity achieved with hydrazine reduction or low-temperature annealing is enough for many device applications. Taking into account the high thermal stability of the widely used and flexible PI substrate, the reduction condition of annealing at 400 °C was carried out overall for the samples studied in our work and the conductivity for the reduced graphene films fabricated on glass, quartz, and PI substrates can reach approximately 10 000 S/m. On the quartz substrate, the graphene film can

be treated at higher temperature and much higher conductivity can be reached. The high conductivity and easy process to obtain conducting flexible graphene films thus could meet the demands for many proposed carbon-based electronics.

A laser system (Spitfire Pro XP, Spectra-Physics) with a central wavelength of 800 nm, a pulse duration of 120 fs, and a repetition rate of 1 kHz was used as the direct-cutting laser to construct our graphene-based patterns and devices, as presented in Figure 1a. During the cutting process, the sample was mounted on computer-controlled translation and rotation stages that move in a programmable step with respect to the laser, and hence the desired patterns could be directly written. Recently, a continuous-wave diode laser was used to etch a GO film to construct an extended area of micropatterned GO (42). However, this diode-laser technique, seriously depending on substrates, has limits in practical use because of the fact that only the GO film but not the much-desired graphene films can be cut. In contrast, through our approach of using a femtosecond laser technique, by accurately tuning the exposure energy of each point (or fluences) and moving the lens and therefore the position of the focus, the power and diameter of the laser spot for cutting graphene films could be easily controlled (49). Namely, not only could the graphene film with different thicknesses on various substrates be cut cleanly and completely with suitable laser parameters but also the width of the etched trenches could be controlled with different exposure energies. These tunable features are vital to fabrication of the electronic circuitry with different architectures and demands. Parts b–d of Figure 1 display a series of scanning electron microscopy (SEM) images of laser direct-cutting patterns for graphene films on different substrates, including flexible PI, glass, and quartz. The dark- and light-gray areas correspond to uncut and cut regions, respectively, and the exposure energy used is all only 16 nJ. Raman spectroscopy performed on the patterned regions of the graphene film on a quartz substrate depicts that the uncut channels display the characteristic graphene D and G bands at 1354 and 1596 cm^{-1} (Figure 1d-1); however, both the D and G bands for the cut area disappear, indicating that no graphene material remains in the trenches after laser direct writing (Figure 1d-2). Moreover, note that from the optical microscope images in Figure 1e–g, with increasing exposure energy (from 16 to 60 nJ), the width (from 1.7 to 4 μm) of the cut channels for graphene films also increases. The exposure energy used for cutting the graphene films was selected to be below or similar to the ablation threshold of the substrates, in order to avoid etching of the substrates.

To further capitalize on this technique with graphene, various simple or complicated graphene-based patterns were fabricated for graphene films on glass, quartz, and flexible PI substrates, as presented in the SEM images of Figure 2. One most notable advantage for this laser direct-writing technique using solution-processed graphene films is that the entire process can be performed in air at ambient conditions and no inert and corrosive gases are needed,

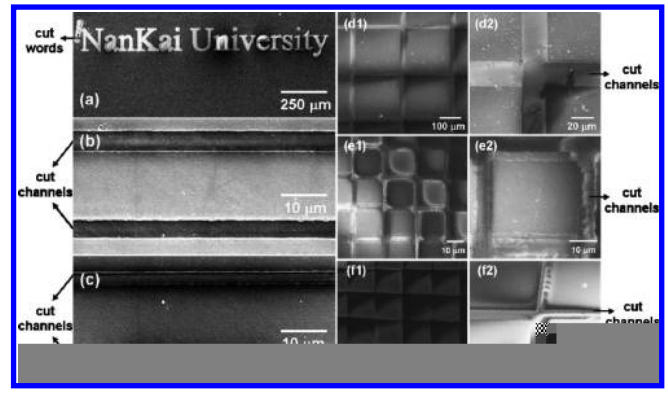

FIGURE 2. (a) SEM image of the words "Nankai University" cut for the graphene film on a quartz substrate. (b and c) SEM images for trenches with different widths cut for the graphene film on a quartz substrate. (d1 and d2) SEM images of square-pillar patterns built by laser direct cutting for the graphene film on a glass substrate. (e1 and e2) SEM images of square-pillar patterns built by laser direct writing for the graphene film on a quartz substrate. (f1 and f2) SEM images of square-pillar patterns built by laser direct cutting for the graphene film on a flexible PI substrate.

different from most of the other techniques/materials. Simple chemistry is behind this advantage because, under a laser beam, the unwanted graphene is turned into volatile gases such as inert CO and CO_2, which run away (42) immediately and leave no remains. This is quite different from the case for metal, silicon, or other inorganic materials (37–49). The cutting of graphene using this technique also has advantages compared with the cutting on organic/polymer films because the organic/polymer material around the edges of the cutting channels may degrade under laser energy, making the material in the entire produced pattern structure not uniform and thus having different properties at different locations. Furthermore, in most cases, toxic gas will be generated for them. With these advantages, in our view, graphene is probably the best material to which to apply this laser direct-cutting/patterning technique to fabricate various micro/nanodevices and electronics directly.

To test whether this approach could be used to fabricate more advanced and complicated electrical circuits and devices directly, we first build an array structure with different sizes of graphene pillars and channels, as shown in Figure 3a on a continuous graphene film. Figure 3b presents the SEM image for the formation of periodic arrays of etched channels and rectangle micropillars in a graphene film. The light- and dark-gray areas correspond to the cut and uncut regions, respectively. The width of these etched trenches is approximately 3 μm, and the dimensions of the rectangle pillars are about 10 μm × 20 μm, denoting that the resolution of the direct-cutting lines can be on the micrometer scale even with our very limited facility (43). Successive cutting can also be applied as displayed in Figure 3c, where one graphene-based rectangle pillar is further cut into two completely separated square pillars. The electrical current with a low voltage of 1.5 V before the laser cutting reaches ~30 μA between points A and B, as shown in Figure 3b. However, after the laser cutting, no current can be detected between points C and D (Figure 3c) using the Keithley 2400 instrument with a sensitivity of 10^{-3} μA. The

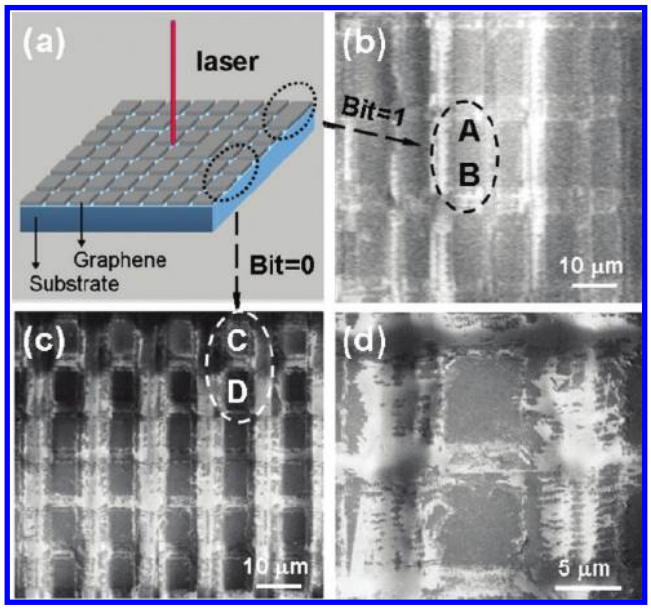

FIGURE 3. (a) Schematic illustration of the process of laser patterning of an array structure with different sizes of graphene pillars and cut channels on a continuous graphene film. (b) Typical SEM image for the array of unwritten rectangle bits (logical "1"). (c) Typical SEM image for the array of pairs of square bits all written with information (logical "0"). (d) Magnified SEM image of a pair of written bits. The thickness of the graphene film is approximately 40 nm.

initial uncut state (thus, as the conducting state, between points A and B shown in Figure 3b) and cut state (thus, as the unconducting state, between points C and D shown in Figure 3c) can correspond to the encode logical "ON" and "OFF" states, which then can be used to store digital data such as logical "1" and "0". The laser-cutting process works as the direct data (bit) writing. Consequently, any information patterned as digital "1" and "0" can be directly written on the graphene films with the computer-controlled laser beam and the ON/OFF ratio can reach a minimum of 10^4. Rather than the common route of encoding logical "1" and "0" for typical memory cards (or the switch ON/OFF mechanism) (50, 51), this novel graphene-based memory card stores data based on conductive or not of the storage bits. Obviously, because of the high chemical stability of graphene and the complete uncut and cut states before and after data writing, the storage data in this approach shall have high reliability and almost infinite lifetime. Moreover, the high chemical stability and environmental compatibility of graphene make these devices withstand any harsh environment. Remarkably, the high scanning speed in our laser direct-writing system, up to 6 mm/s with much higher speeds available, makes this approach an efficient way of producing various real-world electronic devices, including the electrodes for organic photovoltaics (OPV) and light-emitting diode (LED) applications (52, 53).

To demonstrate the real potential of this approach for graphene-based devices, we have further designed and fabricated a prototypical 10-bit WORM memory card (Figure 4) and data-reading system (Figure 5a). Figure 4 illustrates the fabricating process (see methods for details) for this graphene-based prototypical memory card on both glass and flexible PI substrates. As indicated above, high-quality inte-

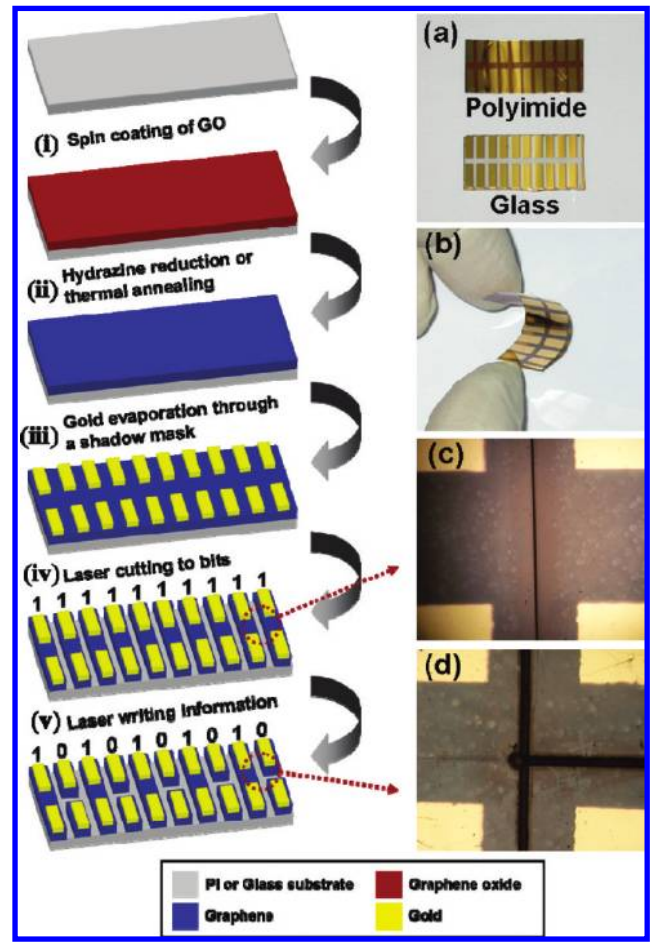

FIGURE 4. Steps i–v: Schematic illustrations and photographs of the fabrication of a prototypical graphene-based WORM memory card with 10 bits. (a) Optical image for graphene films on flexible PI and glass substrates patterned with 10 pairs of gold electrodes. (b) Device on the PI substrate that exhibits well flexibility. (c and d) Optical microscope images of the laser-cutting channels for the prototypical graphene-based WORM memory card on a flexible PI substrate. The light part is the gold electrode, and the black lines are the cut channels.

grated and conductive graphene films are fabricated on the substrates at first (steps I and ii in Figure 4). Then, 10 pairs of gold collecting electrodes with a thickness of 50 nm were evaporated onto the continuous graphene film through a shadow mask, as depicted in step iii of Figure 4. As can be seen, Figure 4a depicts the optical image for graphene films on flexible PI and glass substrates patterned with 10 pairs of gold electrodes. Actually, gold electrodes are not necessary in practical applications because if the proper pattern is made, the graphene itself can be used as the signal/data-collecting electrode directly. Subsequently, laser cutting was applied to cut the continuous graphene film on the substrate into 10 independent bits, each of which contains an independent graphene belt and a pair of two gold electrodes on top, as presented in step iv of Figure 4. This graphene-based bit, which is electrically conductive between the pair of two gold electrodes, corresponds to the graphene rectangle pillar in Figure 3b and is encoded with logical "1". After that, to set any logical "1" bit to the state of "0", the laser is used to etch a channel across this bit between the two collecting electrodes to switch off completely the conductivity between

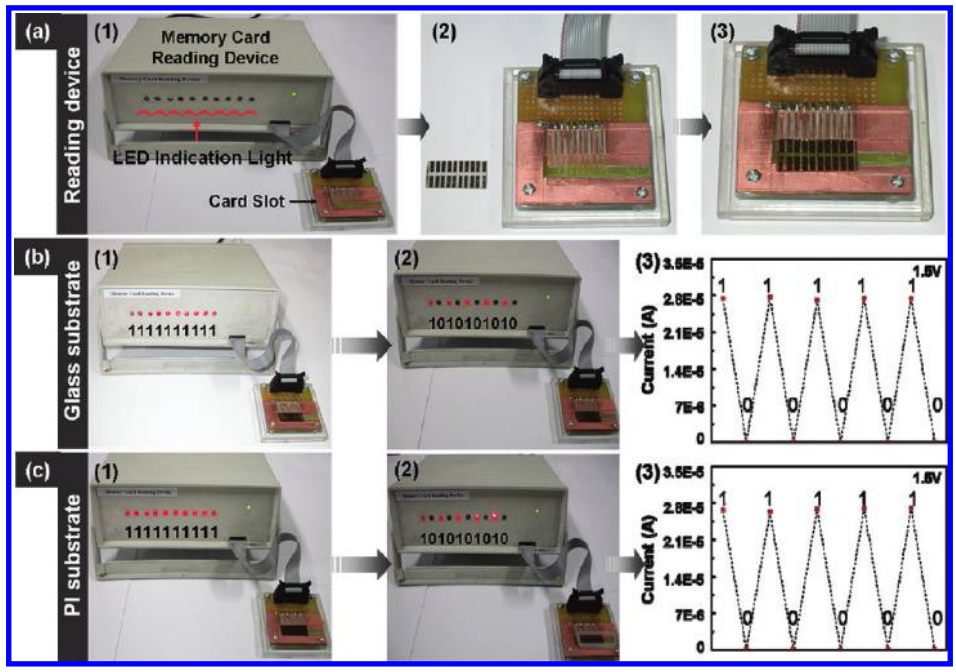

FIGURE 5. (a1) Memory card reading device with 10 independent reading circuitries. Each reading circuitry has an LED indication light to denote whether the corresponding connected bit in the memory card is electrically conductive (logical "1") or not (logical "0"). (a2) Prototype of a memory card with 10 bits and magnified image of the card slot from the reading device. (a3) Memory card plugged into the card slot. (b) Reading process for our archetypal graphene-based WORM memory card on a glass substrate. (b1) When the memory card unwritten with any information fabricated on glass is plugged into the card slot, all 10 LED indication lights are on, indicating that all 10 bits from the memory are electrically conductive (logical "1"). (b2) When the memory card written with information fabricated on glass is plugged into the card slot, the indication lights connecting the written bits are off (logical "0"). (b3) Current−voltage plot for each of the 10 bits from the memory card written with information fabricated on glass. While the bits encoded logical "1" show about 30 μA at a voltage of 1.5 V, the bits encoded logical "0" exhibit electrical insulation. (c) Reading process for our archetypal graphene-based WORM memory card with 10 bits fabricated on a PI substrate, giving the same results as that on a glass substrate.

the two electrodes, equivalent to the pairs of graphene-based square pillars in Figure 3c. As demonstrated in step v of Figure 4, the stored information in logical order of "1" "0" "1" "0" "1" "0" "1" "0" "1" "0" is written in our 10-bit memory device. Parts c and d of Figure 4 present the optical microscope image of the etched channel and intersecting etched channels from the graphene-based memory bits on a flexible PI substrate. It is important to emphasize that these graphene-based memory cards fabricated on PI substrates exhibit outstanding flexibility, as depicted in Figure 4b without any observable downgrade. Moreover, after more than 100 times bending cycles (with bending angle ~ 180°), less than a 2% decrease of the conductivity was observed for this device, which is another good indication of the great flexibility for the graphene-based memory device. These excellent properties are highly demanded for the utility of paperlike storage devices, involving touch-screen, e-tickets/books, and so on.

To demonstrate a complete data writing and reading prototype system, we have also made a demo data-retrieving machine, as presented in Figure 5a1. The reading machine has a card slot and a set of LED indication lights to show the ON/OFF (e.g., "1"/"0") states. The memory cards can be inserted into the card slot to retrieve the written data directly, and the states of "1" or "0" of each bit are indicated by the on and off of the LED light, corresponding to the conducting ("1") and insulating ("0") states of each bit. Figure 5a2 displays the magnified image of the card slot, which is used to connect the memory card with the reading device. The 10 pairs of independent signal-collecting electrodes could be found in the card slot and used to connect with the 10 bits. When the memory card is plugged into the card slot (Figure 5a3), the indication light will be on if the corresponding graphene-based bit is at the ON state, indicating logical "1" is stored; otherwise, the indication light will be off due to the electrical insulation of the corresponding laser written bit (logical "0"). The reading process for our archetypal 10-bit memory cards fabricated on glass and PI substrates is shown in parts b and c of Figure 5, respectively. As expected, all 10 indication lights are on when the unwritten memory cards fabricated on both glass and PI are plugged into the card slot, showing that the stored data are "1" "1" "1" "1" "1" "1" "1" "1" "1" "1" (Figure 5b1,c1). When some bits are switched off to the "0" state, such as data corresponding to "1" "0" "1" "0" "1" "0" "1" "0" "1" "0" stored with laser writing, the stored information can be retrieved as indicated by alternating bright and dark lights in Figure 5b2,c2 from the reading device. Besides, as demonstrated in Figure 5b3,c3, when 1.5 V voltage is applied on the written memory cards prepared on both glass and PI substrates, as in Figure 5b2,c2, ~30 μA current can be detected for the bits alternately. This high ON/OFF ratio also suggests that the architecture for our novel prototype of a graphene-based WORM memory card is indeed feasible and reliable (error-free).

In most cases, one theme common to all WORM memory devices is their requirement of long-time retention of the stored data. The use of graphene, which possesses unprecedented chemical stability under ambient condition, results

in long-time or even permanent data retention for the memory cards. Moreover, it is worth noting that even with our current pattern size, the graphene-based WORM memory card could be fabricated at a storage density up to 500 000 bits/cm^2, enough for the practical use of identification cards, radio-frequency tags, passports, and e-tickets. Actually, it should be very likely that the storage density for this graphene-based WORM memory card could be increased significantly if further optimization is achieved or a much more precise and better cutting technique, such as atomic force microscopy or scanning tunneling microscopy, is used. It should also be noted that other reading mechanisms such as the use of light/laser to retrieve the stored data are very likely because the transparency at each bit is very different before and after laser writing. Finally, the huge advantage of the ability to fabricate all-carbon devices on flexible substrates using the roll-to-roll process makes the dream of having foldable and flexible electrical devices much closer.

CONCLUSION

In summary, we have demonstrated that graphene films, prepared through a simple solution spin-coating process, can be patterned for various microstructures and electronics using a maskless laser direct-writing technique without any post-treatment. The tunable laser beam can completely burn off all layers of graphene in the etched channels and thus can further fabricate all-carbon electronics using graphene films. On the basis of these, a complete working prototype of a flexible WORM memory card coupled with a real data-retrieving system constructed by maskless laser writing to store data directly has been demonstrated. The data density reaches 500 000 bits/cm^2 using our current very limited processing ability, and a much higher data density is expected if current industry-level processing techniques are used. The data storage has a high ON/OFF ratio and almost infinite lifetime. Combing the advantages, including the simple solution process, flexibility, low cost, almost infinite lifetime, and maskless laser data direct-writing method, of this approach, it is fully expected that the dream of fabricating a flexible and foldable all-carbon electronic circuitry is getting a step closer. Most importantly, to our knowledge, no material other than graphene can offer these combined advantages all together to fabricate flexible electronic devices. The possible immediate applications of this approach include electrical wire connections in ICs, identification cards, radio-frequency tags, passports, e-tickets/books, and so on. We fully expect that our results and the exciting perspective for all-carbon devices would prompt more and exciting research and results in this direction.

Acknowledgment. The authors gratefully acknowledge financial support from the NSFC (Grants 50933003, 50902073, 50903044, and 20774047), MOST (Grant 2009AA032304), NSF of Tianjin City (Grant 08JCZDJC25300), and Chinese National Key Basic Research Special Fund (Grant 2006CB921703).

REFERENCES AND NOTES

(1) Novoselov, K. S.; Geim, A. K.; Morozov, S. V.; Jiang, D.; Zhang, Y.; Dubonos, S. V.; Grigorieva, I. V.; Firsov, A. A. *Science* **2004**, *36*, 666–669.
(2) Avouris, P.; Chen, Z. H.; Perebeinos, V. *Nat. Nanotechnol.* **2007**, *2*, 605–615.
(3) Balandin, A. A.; Ghosh, S.; Bao, W. Z.; Calizo, I.; Teweldebrhan, D.; Miao, F.; Lau, C. N. *Nano Lett.* **2008**, *8*, 902–907.
(4) Booth, T. J.; Blake, P.; Nair, R. R.; Jiang, D.; Hill, E. W.; Bangert, U.; Bleloch, A.; Gass, M.; Novoselov, K. S.; Katsnelson, M. I.; Geim, A. K. *Nano Lett.* **2008**, *8*, 2442–2446.
(5) Lee, C.; Wei, X. D.; Kysar, J. W.; Hone, J. *Science* **2008**, *321*, 385–388.
(6) Nair, R. R.; Blake, P.; Grigorenko, A. N.; Novoselov, K. S.; Booth, T. J.; Stauber, T.; Peres, N. M. R.; Geim, A. K. *Science* **2008**, *320*, 1308.
(7) Meyer, J. C.; Geim, A. K.; Katsnelson, M. I.; Novoselov, K. S.; Booth, T. J.; Roth, S. *Nature* **2007**, *446*, 60–63.
(8) Gao, W.; Alemany, L. B.; Ci, L. J.; Ajayan, P. M. *Nat. Chem.* **2009**, *1*, 403–408.
(9) Stankovich, S.; Dikin, D. A.; Dommett, G. H. B.; Kohlhaas, K. M.; Zimney, E. J.; Stach, E. A.; Piner, R. D.; Nguyen, S. T.; Ruoff, R. S. *Nature* **2006**, *442*, 282–286.
(10) Liang, J. J.; Huang, Y.; Zhang, L.; Wang, Y.; Ma, Y. F.; Guo, T. Y.; Chen, Y. S. *Adv. Funct. Mater.* **2009**, *19*, 2297–2302.
(11) Ramanathan, T.; Abdala, A. A.; Stankovich, S.; Dikin, D. A.; Herrera-Alonso, M.; Piner, R. D.; Adamson, D. H.; Schniepp, H. C.; Chen, X.; Ruoff, R. S.; Nguyen, S. T.; Aksay, I. A.; Prud'homme, R. K.; Brinson, L. C. *Nat. Nanotechnol.* **2008**, *3*, 327–331.
(12) Zhou, X. Z.; Huang, X.; Qi, X. Y.; Wu, S. X.; Xue, C.; Boey, F.; Yan, Q. Y.; Chen, P.; Zhang, H. *J. Phys. Chem. C* **2009**, *113*, 10842–10846.
(13) Huang, X.; Zhou, X. Z.; Wu, S. X.; Wei, Y. Y.; Qi, X. Y.; Zhang, J.; Boey, F.; Zhang, H. *Small* **2010**, *6*, 513–516.
(14) Qi, X. Y.; Pu, K. Y.; Zhou, X. Z.; Li, H.; Liu, B.; Boey, F.; Huang, W.; Zhang, H. *Small* **2010**, *6*, 663–669.
(15) Becerril, H. A.; Mao, J.; Liu, Z.; Stoltenberg, R. M.; Bao, Z.; Chen, Y. *ACS Nano* **2008**, *2*, 463–470.
(16) Li, X. L.; Zhang, G. Y.; Bai, X. D.; Sun, X. M.; Wang, X. R.; Wang, E.; Dai, H. J. *Nat. Nanotechnol.* **2008**, *3*, 538–542.
(17) Kim, K. S.; Zhao, Y.; Jang, H.; Lee, S. Y.; Kim, J. M.; Kim, K. S.; Ahn, J. H.; Kim, P.; Choi, J. Y.; Hong, B. H. *Nature* **2009**, *457*, 706–710.
(18) Wang, X.; Zhi, L. J.; Tsao, N.; Tomovic, Z.; Li, J. L.; Mullen, K. *Angew. Chem., Int. Ed.* **2008**, *47*, 2990–2992.
(19) Li, B.; Cao, X. H.; Ong, H. K.; Cheah, J. W.; Zhou, X. Z.; Yin, Z. Y.; Li, H.; Wang, J. L.; Boey, F.; Huang, W.; Zhang, H. *Adv. Mater.* **2010**, *22*, 3058–3061.
(20) Liu, J. Q.; Lin, Z. Q.; Liu, T. J.; Yin, Z. Y.; Chen, S. F.; Xie, L. H.; Boey, F.; Zhang, H.; Huang, W. *Small* **2010**, *6*, 1536–1542.
(21) Yin, Z. Y.; Wu, S. X.; Zhou, X. Z.; Huang, X.; Zhang, Q. C.; Boey, F.; Zhang, H. *Small* **2010**, *6*, 307–312.
(22) Robinson, J. T.; Perkins, F. K.; Snow, E. S.; Wei, Z. Q.; Sheehan, P. E. *Nano Lett.* **2008**, *8*, 3137–3140.
(23) Schedin, F.; Geim, A. K.; Morozov, S. V.; Hill, E. W.; Blake, P.; Katsnelson, M. I.; Novoselov, K. S. *Nat. Mater.* **2007**, *6*, 652–655.
(24) He, Q. Y.; Sudibya, H. G.; Yin, Z. Y.; Wu, S. X.; Li, H.; Boey, F.; Huang, W.; Chen, P.; Zhang, *ACS Nano* **2010**, *4*, 3201–3208.
(25) Wang, Z. J.; Zhou, X. Z.; Zhang, J.; Boey, F.; Zhang, H. *J. Phys. Chem. C* **2009**, *113*, 14071–14075.
(26) Stoller, M. D.; Park, S. J.; Zhu, Y. W.; An, J. H.; Ruoff, R. S. *Nano Lett.* **2008**, *8*, 3498–3502.
(27) Wang, Y.; Shi, Z. Q.; Huang, Y.; Ma, Y. F.; Wang, C. Y.; Chen, M. M.; Chen, Y. S. *J. Phys. Chem. C* **2009**, *113*, 13103–13107.
(28) Yoo, E.; Kim, J.; Hosono, E.; Zhou, H.; Kudo, T.; Honma, I. *Nano Lett.* **2008**, *8*, 2277–2282.
(29) Das, A.; Pisana, S.; Chakraborty, B.; Piscanec, S.; Saha, S. K.; Waghmare, U. V.; Novoselov, K. S.; Krishnamurthy, H. R.; Geim, A. K.; Ferrari, A. C.; Sood, A. K. *Nat. Nanotechnol.* **2008**, *3*, 210–215.
(30) Eda, G.; Fanchini, G.; Chhowalla, M. *Nat. Nanotechnol.* **2008**, *3*, 270–274.
(31) Briseno, A. L.; Mannsfeld, S. C. B.; Ling, M. M.; Liu, S. H.; Tseng, R. J.; Reese, C.; Roberts, M. E.; Yang, Y.; Wudl, F.; Bao, Z. N. *Nature* **2006**, *444*, 913–917.
(32) Ozin, G. A. *Adv. Mater.* **1992**, *4*, 612–649.
(33) Liang, X.; Fu, Z.; Chou, S. Y. *Nano Lett.* **2007**, *7*, 3840–3844.
(34) Reina, A.; Jia, X. T.; Ho, J.; Nezich, D.; Son, H. B.; Bulovic, V.; Dresselhaus, M. S.; Kong, J. *Nano Lett.* **2009**, *9*, 30–35.
(35) Chen, J. H.; Ishigami, M.; Jang, C.; Hines, D. R.; Fuhrer, M. S.; Williams, E. D. *Adv. Mater.* **2007**, *19*, 3623–3627.

(36) Campos-Delgado, J.; Romo-Herrera, J. M.; Jia, X. T.; Cullen, D. A.; Muramatsu, H.; Kim, Y. A.; Hayashi, T.; Ren, Z. F.; Smith, D. J.; Okuno, Y.; Ohba, T.; Kanoh, H.; Kaneko, K.; Endo, M.; Terrones, H.; Dresselhaus, M. S.; Terrones, M. *Nano Lett.* **2008**, *8*, 2773–2778.
(37) Hirata, M.; Gotou, T.; Horiuchi, S.; Fujiwara, M.; Ohba, M. *Carbon* **2004**, *42*, 2929–2937.
(38) Niyogi, S.; Bekyarova, E.; Itkis, M. E.; McWilliams, J. L.; Hamon, M. A.; Haddon, R. C. *J. Am. Chem. Soc.* **2006**, *128*, 7720–7721.
(39) Shen, J. F.; Hu, Y. H.; Li, C.; Qin, C.; Ye, M. X. *Small* **2009**, *5*, 82–85.
(40) Stankovich, S.; Piner, R. D.; Nguyen, S. T.; Ruoff, R. S. *Carbon* **2006**, *44*, 3342–3347.
(41) Lim, K. Y.; Sow, C. H.; Lin, J. Y.; Cheong, F. C.; Shen, Z. X.; Thong, J. T. L.; Chin, K. C.; Wee, A. T. S. *Adv. Mater.* **2003**, *15* (4), 300–303.
(42) Zhou, D. B.; Bao, Q. L.; Varghese, B.; Tang, L. A. L.; Tan, C. K.; Sow, C. H.; Loh, K. P. *Adv. Mater.* **2010**, *22*, 67–71.
(43) Chrisey, D. B. *Science* **2000**, *289*, 879–881.
(44) Her, T. H.; Finlay, R. J.; Wu, C.; Deliwala, S.; Mazur, E. *Appl. Phys. Lett.* **1998**, *73*, 1673–1675.
(45) Ehrlich, D. J.; Osgood, R. M.; Deutsch, T. F. *Appl. Phys. Lett.* **1981**, *38*, 1018–1020.
(46) Eldada, L.; Xu, C. Z.; Stengel, K. M. T.; Shacklette, L. W.; Yardley, J. T. *J. Lightwave Technol.* **1996**, *14*, 1704–1713.
(47) Wilson, O.; Wilson, G. J.; Mulvaney, P. *Adv. Mater.* **2002**, *14*, 1000–1004.
(48) Ozkan, A. M.; Malshe, A. P.; Railkar, T. A.; Brown, W. D.; Shirk, M. D.; Molian, P. A. *Appl. Phys. Lett.* **1999**, *75*, 3716–3718.
(49) Baldacchini, T.; Carey, J. E.; Zhou, M.; Mazur, E. *Langmuir* **2006**, *22*, 4917–4919.
(50) Ling, Q. D.; Song, Y.; Lim, S. L.; Teo, E. Y. H.; Tan, Y. P.; Zhu, C. X.; Chan, D. S. H.; Kwong, D. L.; Kang, E. T.; Neoh, K. G. *Angew. Chem., Int. Ed.* **2006**, *45*, 2947–2451.
(51) Moller, S.; Perlov, C.; Jackson, W.; Taussig, C.; Forrest, S. R. *Nature* **2003**, *426*, 166–169.
(52) Liu, Z. F.; Liu, Q.; Huang, Y.; Ma, Y. F.; Yin, S. G.; Zhang, X. Y.; Sun, W.; Chen, Y. S. *Adv. Mater.* **2008**, *20*, 3924–3930.
(53) Xu, Y. F.; Long, G.; Huang, L.; Huang, Y.; Wan, X. J.; Ma, Y. F.; Chen, Y. S. *Carbon* **2010**, *48*, 3308–3311.

AM1007326